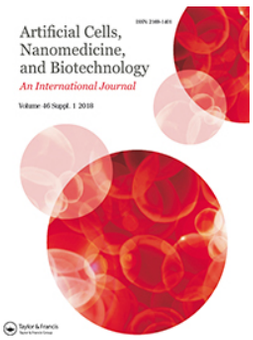

Taylor & Francis
Taylor & Francis Group

Artificial Cells, Nanomedicine, and Biotechnology

An International Journal

ISSN: 2169-1401 (Print) 2169-141X (Online) Journal homepage: https://www.tandfonline.com/loi/ianb20

Controlled release of mitomycin C from PHEMAH–Cu(II) cryogel membranes

Monireh Bakhshpour, Handan Yavuz & Adil Denizli

To cite this article: Monireh Bakhshpour, Handan Yavuz & Adil Denizli (2018) Controlled release of mitomycin C from PHEMAH–Cu(II) cryogel membranes, Artificial Cells, Nanomedicine, and Biotechnology, 46:sup1, 946-954, DOI: 10.1080/21691401.2018.1439840

To link to this article: https://doi.org/10.1080/21691401.2018.1439840

ARTIFICIAL CELLS, NANOMEDICINE, AND BIOTECHNOLOGY
2018, VOL. 46, NO. S1, S946–S954
https://doi.org/10.1080/21691401.2018.1439840

Controlled release of mitomycin C from PHEMAH–Cu(II) cryogel membranes

Monireh Bakhshpour, Handan Yavuz and Adil Denizli

Department of Chemistry, Hacettepe University, Ankara, Turkey

ABSTRACT

Molecular imprinting technique was used for the preparation of antibiotic and anti-neoplastic chemotherapy drug (mitomycin C) imprinted cryogel membranes (MMC-ICM). The membranes were synthezied by using metal ion coordination interactions with *N*-methacryloyl-(L)-histidine methyl ester (MAH) functional monomer and template molecules (i.e. MMC). The 2-hydroxyethyl methacrylate (HEMA) monomer and methylene bisacrylamide (MBAAm) crosslinker were used for the preparation of mitomycin C imprinted cryogel membranes by radical suspension polymerization technique. The imprinted cryogel membranes were characterized by scanning electron microscopy (SEM), Brunauer–Emmett–Teller (BET), Fourier transform infrared spectroscopy-attenuated total reflectance (FTIR-ATR) and swelling degree measurements. Cytotoxicity of MMC-ICMs was investigated using mouse fibroblast cell line L929. Time-dependent release of MMC was demonstrated within 150 h from cryogel membranes. Cryogels demonstrated very high MMC loading efficiency (70–80%) and sustained MMC release over hours.

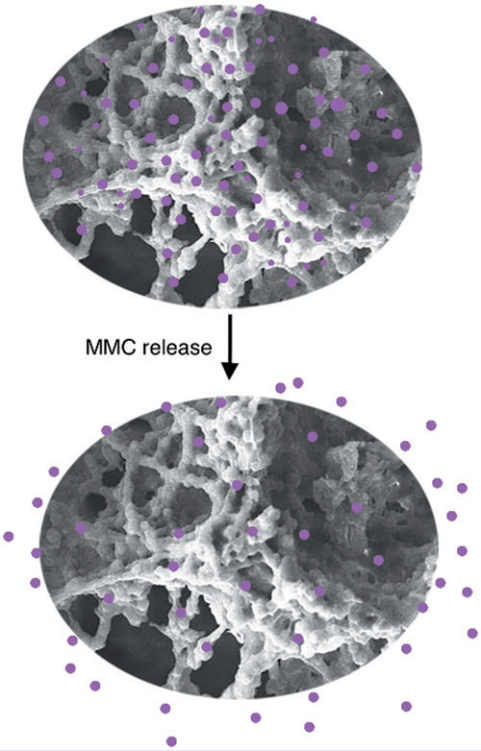

ARTICLE HISTORY
Received 9 December 2017
Revised 7 February 2018
Accepted 8 February 2018

KEYWORDS
Mitomycin C; controlled release; molecular imprinting; cryogel membrane

Introduction

Drug delivery is a technology that leads to release of the drug in the range of therapeutic window. Smart drug delivery systems have drawn the attention of scientists, biomedical and pharmaceutical fields in recent years [1] The aim of drug delivery systems is to increase the efficacy and safety of drug treatment, release the convenient therapeutic dosage of the drug into the body, reduce the side effects, keep the pharmacological effect of the coadministration of drug and provide a minimum dose to the patient for a long time [2–4].

Mitomycin C (MMC) is a DNA alkylating agent and used in chemotherapeutic treatments owing to its non-specific antitumor activity. MMC is a natural product obtained from the

CONTACT Adil Denizli denizli@hacettepe.edu.tr Hacettepe University, Department of Chemistry, Biochemistry Division, Ankara, Turkey

culture medium of *Streptomyces caespitosus*. MMC has been used alone or in combination with other chemotherapeutic agents in the treatment of gastrointestinal, lung, uterus, head and neck, pancreas and bladder cancer and chronic leukemia [5]. MMC shows antitumor effect by inhibiting DNA replication as it binds to the DNA in tumor cells by forming cross-links between the two arms of the DNA double helix [6,7]. MMC has a number of acute and chronic toxicities that limits its use in the clinical applications. Various delivery methods have been shown to lessen the toxic effects of MMC. One of the most efficient approaches for the drug delivery is molecular imprinting method [8,9].

Molecular imprinting (MI) method encompass design and synthesis of novel materials which are capable of recognizing proteins and other biological assemblies, such as whole cells and viruses and have potential fundamental and practical applications [10–13]. Specific applications of such materials include down-stream bioprocess for the purification of biopharmaceuticals, drug delivery, diagnostics, sensors, etc. [14–18]. Molecular imprinting method, which is based on matching spatial distribution of complementary functional groups on the surface of receptor polymers to those of target molecules, has been largely confined to small organic molecules as the substrates [19]. The molecule of interest is allowed to interact with functional monomers via covalent [20], non-covalent [21] or metal ion coordination [22] interactions. Generally, the studies for drug delivery by MI have investigated non-covalent interactions that can be insufficient for drug delivery systems [23,24]. Metal ion coordination imprinting is an alternative approach for the weak non-covalent interactions [22]. Metal ion coordination has higher strength with respect to hydrogen bonding, which makes it more stable in aqueous media [25]. Additionally, metal ion coordination is a fast binding process and binding strength can be adjusted by choosing appropriate metal ion for a defined template molecule. Furthermore, it is possible to replace the metal ion with another one to enhance the selectivity or use of the molecular imprinted polymer for different purposes [15,16,26]. Therefore, metal ion coordination approach has an important potential for preparation of highly specific molecular imprinting polymers in aqueous medium. Recently, the molecular imprinting method has gained increasing attention for drugs, amino acids, peptides, hormones and proteins [27–29] as it results in slow and longer release of therapeutic drugs and strengthens the loading capacity.

Cryogels are macroporous polymeric gels, synthesized by cryotropic gelation [30]. Pore dimension of cryogels changing between 10th fractions of micrometer to hundreds of micrometers, chemical and mechanical stabilities make them useful for biotechnological and biomedical applications such as carriers for enzyme immobilization, microbial cell and antibody immobilization, gel bases for bioaffinity sorbent and drug delivery systems [31–37].

The aim of this study was to prepare MMC imprinted poly(hydroxyethyl methacrylate-*N*-methacryloyl-(L)-histidine methyl ester)–Cu(II) [PHEMAH–Cu(II)] cyrogel membranes for controlled delivery of MMC. *N*-Methacryloyl-(L)-histidine methyl ester (MAH) was chosen as a functional monomer and the MMC molecules were complexed through chelation with Cu(II) ions. Then, MMC-PHEMAH–Cu(II) cyrogel membranes (MMC-ICMs) were prepared and characterized thoroughly and delivery experiments were studied *in vitro*. There, the effects of MMC loading ratio, amount of cross linker and temperature of polymerization on the MMC delivery rate were determined in PBS buffer at 37 °C.

Table 1. Parameters for cryogel membrane synthesis.

Notation for cryogels	(μg) MMC/ g polymer	n_{HEMA}/n_{MBAAm}	Polymerization temperature (°C)
MMC-ICM1	50	1:16	−14
MMC-ICM2	50	1:10	−14
MMC-ICM3	50	1:8	−14
MMC-ICM4	50	1:4	−14
MMC-ICM5	50	1:4	−18
MMC-ICM6	50	1:4	−20
MMC-ICM7	50	1:4	−24
NICM	0	1:4	−14
PHEMACM	0	1:4	−14

Experimental

Materials

2-Hydroxyethyl methacrylate (HEMA), ammonium persulphate (APS), methylene bisacrylamide (MBAAm), and *N*,*N*,*N*′,*N*′-tetramethylene diamine (TEMED) were purchased from Sigma Chemical Co. (St. Louis, MO). Mitomycin C (MMC) was obtained from Kyowa, Hakko Kogyo Co Ltd. (Tokyo, Japan). *N*-Methacryloyl-(L)-histidine methyl ester (MAH) monomer was purchased from NanoReg (Ankara, Turkey). All other chemicals were of reagent grade and were purchased from Merck AG (Darmstadt, Germany). Deionized water (DW) was obtained from millipore Simplicity 185 Ultrapure Water System.

Preparation of MMC-ICMs

The membranes used in this study can be divided into nine parts as MMC-ICM1, MMC-ICM2, MMC-ICM3, MMC-ICM4, MMC-ICM5, MMC-ICM6, MMC-ICM7, NICM, PHEMACM with respect to the amount of cross-linker, template and other polymerization conditions (Table 1). First, the pre-polymerization complex of MAH–Cu(II)–MMC was prepared by mixing 0.01 mmol of MAH, 0.01 mmol of copper ions (source: $Cu(NO_3)_2.5\,H_2O$), and 1 ml of MMC solution at pH 7.4 (phosphate-buffered saline, PBS, buffer) for 1 h at room temperature under stirring. The formation of MAH–Cu(II) and MAH–Cu(II)–MMC complexes were observed with UV–vis spectrophotometer and recorded between 220 and 600 nm (Shimadzu UV-1601, Shimadzu Corp, Kyoto, Japan). In the second step, the main monomer HEMA and MBAAm as cross-linker was dissolved in 13.8 ml of DW and then MAH–Cu(II)–MMC complex was added. Then, the mixture was degassed by passing nitrogen gas. The cryogel membranes were synthesized by free radical polymerization initiated by APS and TEMED. The solution was frozen at −14 °C for 24 h. After melting of ice crystals in the cryogel structure, the resulting cryogel membrane was washed with DW, and cut into circular pieces with 2.2 cm to produce MMC-ICMs1. Non-imprinted PHEMAH cryogel membranes (NICMs) were

prepared as described above without MMC. The PHEMA cryogel membranes (PHEMACMs) were also prepared for control of MAH–Cu(II) effect in to the MMC delivery. Polymerization recipe is given in Table 1. The removal of the MMC molecules from the cryogel network was achieved using 0.5 M NaCl for 2 h at 25 °C.

Characterization of MMC-ICMs

The chemical structure of MMC-ICMs was characterized by Fourier transform infrared spectroscopy-attenuated total reflectance (FTIR-ATR) spectroscopy (Thermo Fisher Scientific, Nicolet is10, Waltham, MA, USA). The surface morphology of the cryogel membranes was examined by using scanning electron microscopy (SEM, Zeiss Supra55, Germany). The specific surface area of cryogel membranes was measured according to the Brunauer–Emmett–Teller (BET) model using multi point analysis (Flowsorb II 2300 from Micromeritics Instrument Corporation, Norcross, GA). The swelling degree (S) of cryogels was performed in water. The cryogels were placed in distilled water until constant weight. The mass of wet ($m_{\text{wet gel}}$) and dry ($m_{\text{dry gel}}$) cryogels were recorded and the swelling degree was calculated according to the following equation:

$$\text{Swelling Degree } (\%) = [(m_{\text{wet gel}} - m_{\text{dry gel}})/m_{\text{dry gel}}] \times 100 \quad (1)$$

In vitro MMC delivery studies

The MMC loaded MMC-ICMs were dried and then MMC delivery studies were investigated in 5 ml of PBS buffer, pH 7.4 at 37 °C. At predetermined time intervals, a specific volume of release media was taken out and an equal volume of fresh media was added to the release medium. Cu(II) leakage from PHEMAH cryogel membranes was investigated with a graphite furnace atomic absorption spectrometer (Analyst 800/Perkin-Elmer, Shelton, CT). All results related to medium and drug transport behavior were obtained for $n = 3$ and the mean values were expressed. The crosslinker content in polymer is one of the important factors affecting the release rate. The continuous MMC delivery from MMC-ICM1, MMC-ICM2, MMC-ICM3, MMC-ICM4 with 1:16, 1:10, 1:8 and 1:4 molar ratio of $n_{\text{HEMA}}/n_{\text{MBAAm}}$, respectively, and MMC-ICM4, MMC-ICM5, MMC-ICM6, MMC-ICM7 synthesized at −14, −18, −20, −22 °C, respectively, was investigated to observe the monomer/crosslinker and polymerization temperature effect. These parameters are affective on pore size and structure of the cyrogel membranes and, therefore, affect the release of MMC. MMC-ICM4 was studied for different MMC concentrations (i.e. 50, 75, 100 and 200 μg MMC/mL pH: 7.4 PBS buffer). The concentration of MMC was measured at 365 nm using UV/Vis spectrophotometer (Shimadzu, Model 1601, Tokyo, Japan).

In vitro cytotoxicity tests for MMC-ICMs

Cytotoxic effects of MMC-ICMs were investigated based on the ISO-10993-5 'Biological Evaluation of Medical Devices' standards by the 3-(4,5-dimethyl/thiazol-2-yl) 2,5-diphenyltetrazolium bromide thiazolyl blue (MTT) test. Cytotoxicity was studied by using fibroblast cell line (L929). Cells were cultured in a medium containing DMEM supplemented with 10% foetal bovine serum and 10% L-glutamine in a humidified atmosphere of 95% air and 5% CO_2 at 37 °C for 3 d. MMC-ICMs were sterilized under ultraviolet light for 1 h and incubated for 72 h in cell culture medium at 37 °C. L929 cells at a density of 1×10^3 per well were cultured in a 200 μL volume of cell culture medium in a 96 well cell plate and incubated overnight in humidified 5% CO_2. After that, cell culture medium was replaced with extract medium and incubated at 37 °C for 24 h. Then cultured cells were treated with 100 μL/well MTT solution for 4 h. Then, plates were incubated at dark at room temperature for 30 min. Finally, they were read by an automatic enzyme-linked immunosorbent assay (ELISA) reader at 540 nm.

Results and discussion

Characterization of MMC-ICMs

MAH monomer was used as a metal-chelating ligand for Cu(II)-mediated coordination. The imidazole group can easily form coordination bonds with transition metal ions due to the Lewis base character of the nitrogen atoms in the heteroaromatic ring. Figure 1(A) shows the chemical structure of MAH monomer and Figure 1(B) shows UV–vis spectra of MAH, MAH–Cu(II) and MAH–Cu(II)–MMC complexes in 1:1 molar ratio. The decrement of band absorbances represents interaction between MAH–Cu(II) and MMC. Hypothetical model for the MAH–Cu(II)–MMC was shown in Figure 1(C). It should be noted that there was no Cu(II) leakage from MMC-ICMs which implies that Cu(II) ions were chelated strongly with MAH.

FTIR-ATR spectrum of MMC-ICM shows amide bands at 1716 cm^{-1}, 1621 cm^{-1} (Figure 2). The value 3100–3000 cm^{-1} corresponds to the aromatic and aliphatic C–H streching bands. The broad bands presenting in the region of 3400–3200 cm^{-1} correspond to the O–H streching bands of HEMA in the MMC-ICM. The presence of the amide bands in the FTIR-ATR spectra indicates the incorporation of the metal-chelating monomers in the structure of MMC-ICM.

The surface morphology of the MMC-ICM was exemplified by SEM. The cryogel membranes were synthesized at different polymerization temperatures and monomer/crosslinker ratios, to observe their effect on pore size and structure. Figure 3(A–D) shows the structure of cryogels that synthesized at −14, −18, −20, −22 °C polymerization temperatures. As seen in these figures, the pore size of the cryogel membranes increased with increasing polymerization temperature. To produce small crystals, freezing should be at a very low temperature and freezing rate should be high to reduce the time available for ice crystals to grow. Because solvent crystals in the cryogelation systems act as template for the formation of pores, the same relationship usually exists between the pore size of cyrogels and the polymerization temperature.

The effect of crosslinker is shown in Figure 4(A–D) that is 1:16, 1:10, 1:8 and 1:4 molar ratio of $n_{\text{HEMA}}/n_{\text{MBAAm}}$, respectively. SEM pictures were showed that cryogel membranes have interconnected macropores in diameters from

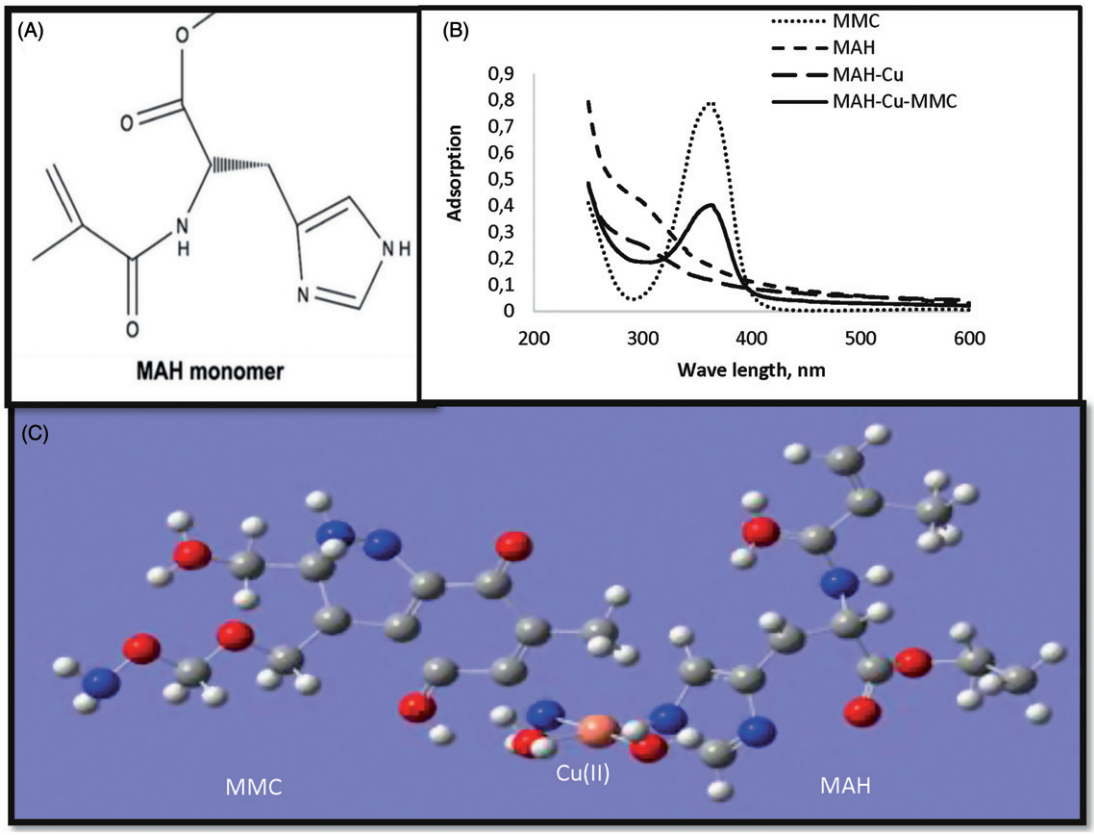

Figure 1. (A) The structure of MAH monomer. (B) The UV-spectrum of MAH–Cu(II)–MMC complex. (C) Hypothetical model for the MAH–Cu(II)–MMC complex.

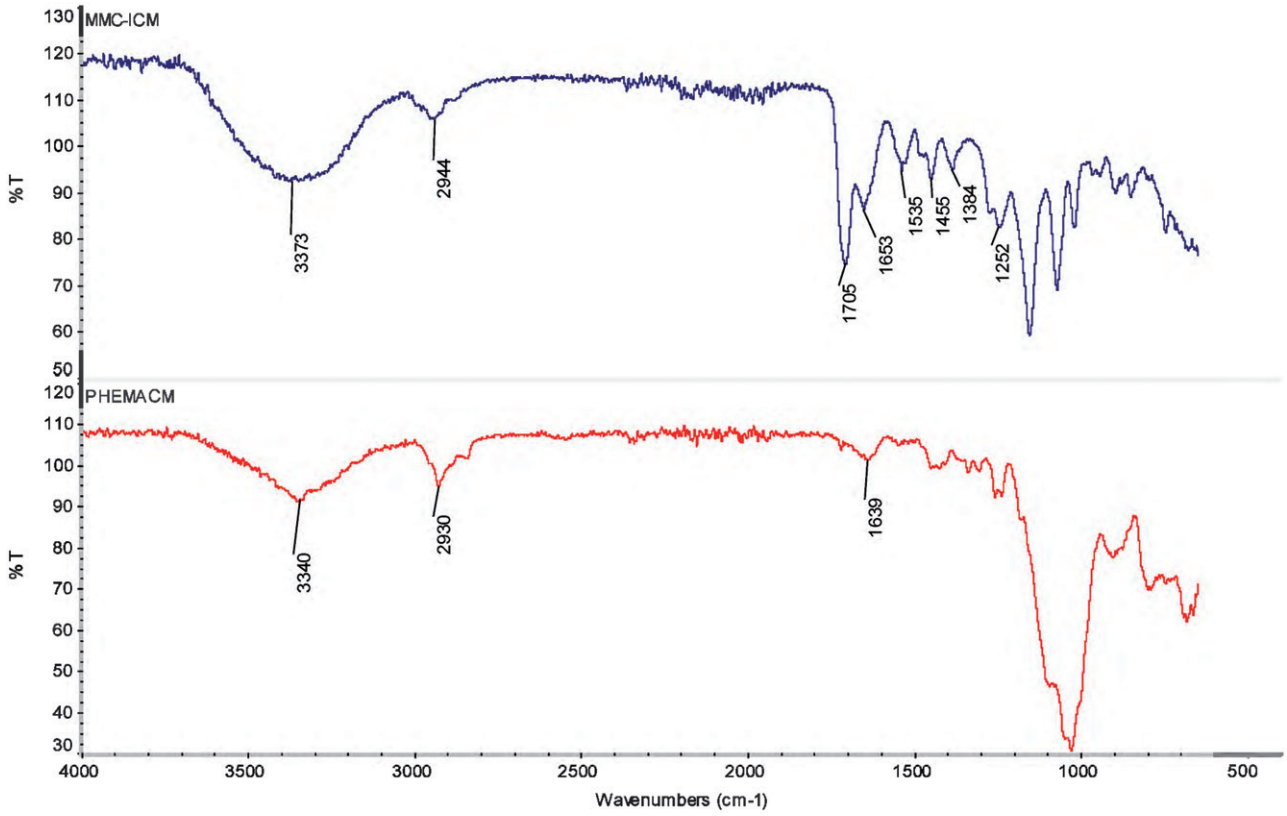

Figure 2. FTIR-ATR spectra of MMC-ICM and PHEMACM.

10 to 100 μm. Larger cross-linker ratios reduced the size of macropores, thereby reduced the pore size of cyrogels. It was observed that the release rate and the amount of MMC released from cryogels decreased with increasing the cross-linker ratio. The high reversibility of these macroporous cryogel could be very useful in the field of

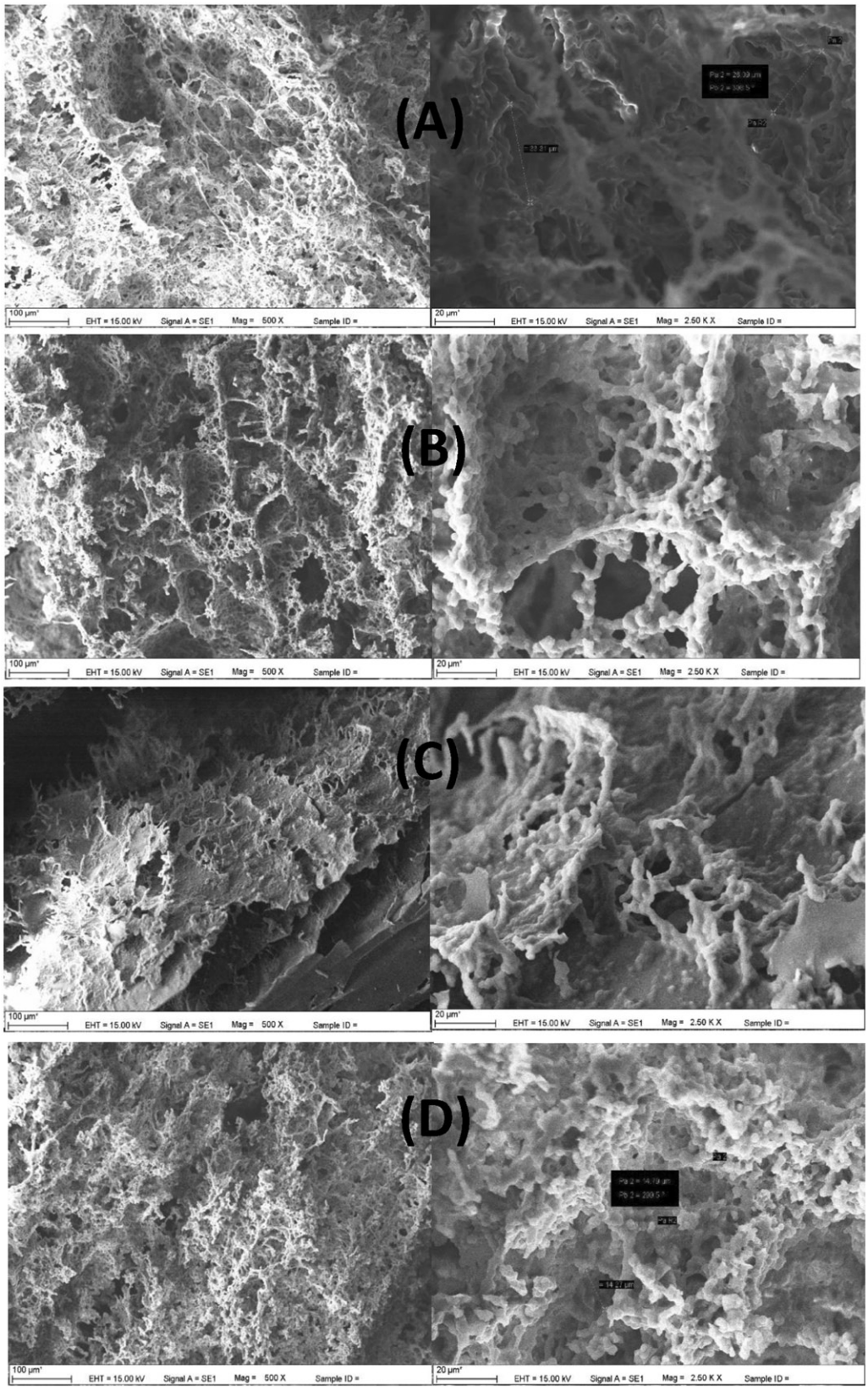

Figure 3. The SEM images of MMC-ICMs synthesized at (A) − 14 °C, (B) − 18 °C, (C) − 20 °C and (D) − 22 °C.

biomaterials and biotechnology [38]. Effects of the temperature and the initial monomer concentration on the porosity properties of cryogels have been studied intensively [39].

As we know, cryogels are perfect materials for chromatographic separation. Cryogels have perfect flow dynamics and work well with viscous liquids. The cryogels can be also used for drug delivery systems. Appropriate cross-linkers are widely

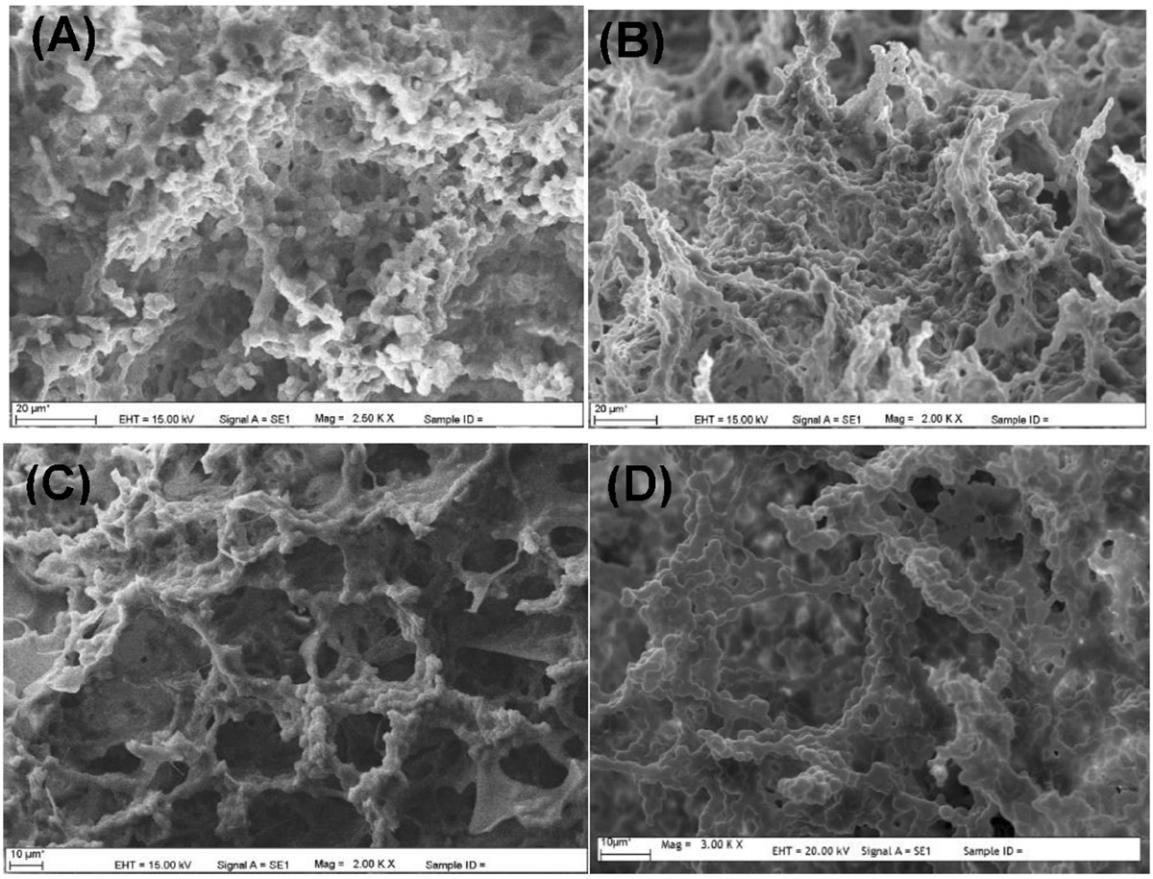

Figure 4. The SEM photograph of MMC-ICMs synthesized with different monomer ratios at −14 °C: (A) 1:16, (B) 1:10, (C) 1:8 and (D) 1:4 n_{HEMA}/n_{MBAAm}.

Table 2. Comparison of the properties of cryogel membranes.

Notation for cryogels	n_{HEMA}/n_{MBAAm}	Polymerization temperature (°C)	Swelling ratio %	Surface area m^2/g	Pore diameter (μm)
MMC-ICM1	1:16	−14	757.9 ± 0.1	30.8	20–50
MMC-ICM2	1:10	−14	761.2 ± 0.1	33.3	
MMC-ICM3	1:8	−14	803.5 ± 0.1	35.5	
MMC-ICM4	1:4	−14	898.4 ± 0.1	45.2	
MMC-ICM5	1:4	−18	831.3 ± 0.1	38.1	
MMC-ICM6	1:4	−20	789.1 ± 0.1	33.6	
MMC-ICM7	1:4	−24	769.1 ± 0.1	30.2	
N-ICM	1:4	−14	705.2 ± 0.1	21.6	

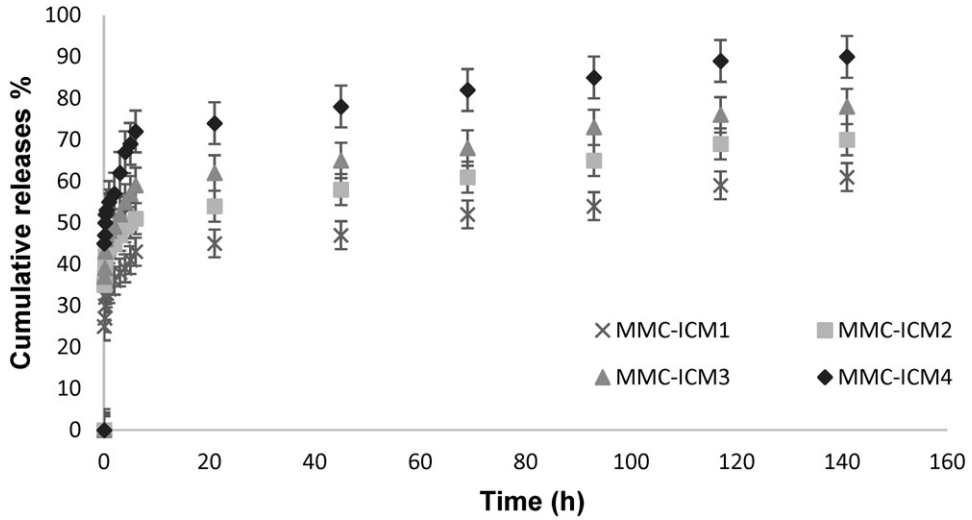

Figure 5. Effect of cross-linker ratio on the MMC release (BPS buffer, 37 °C, $n = 3$).

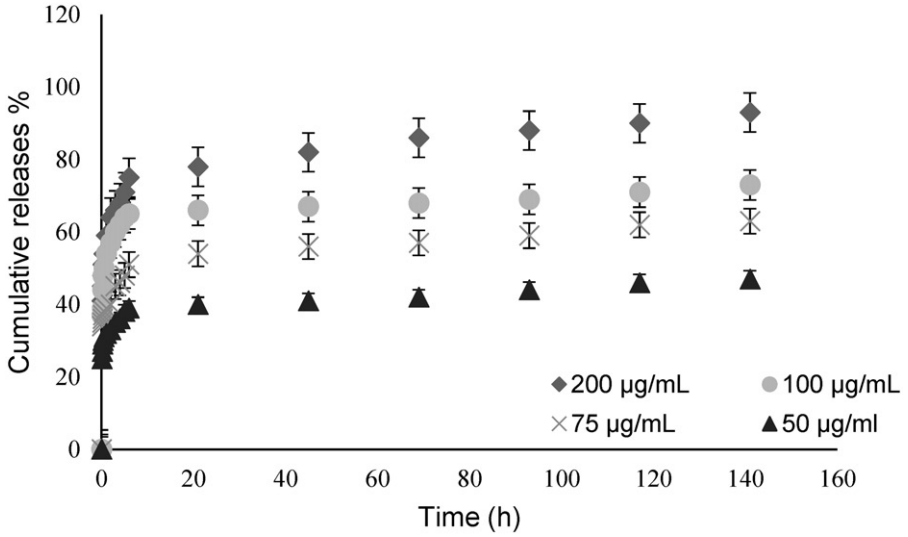

Figure 6. Effect of loaded drug concentration on the MMC release from MMC-ICM4.

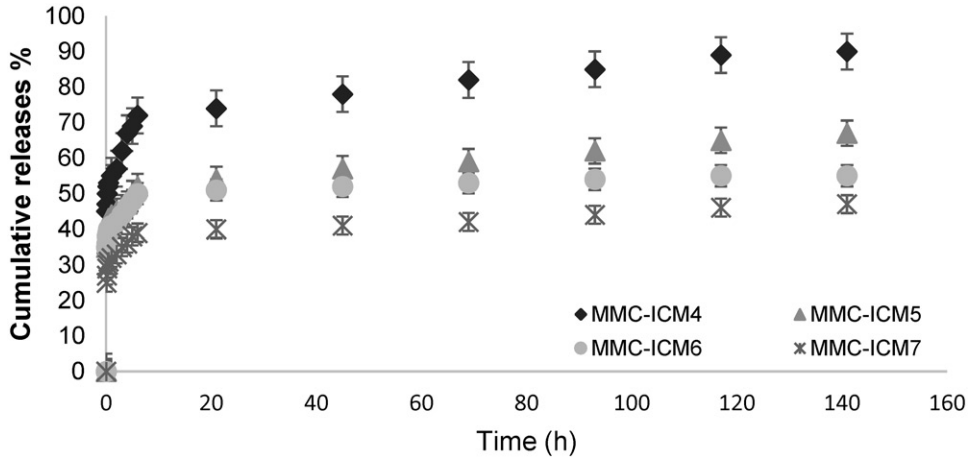

Figure 7. Effect of polymerization temperature on MMC delivery from the cryogel membranes.

used to prepare macroporous cryogels. Macroporous structures can be designed by controlling the content of cross-linker and the conditions of polymerization. Table 2 shows the pore size of cryogels synthesized at different conditions in this study.

The equilibrium degree of swelling is an important property of membranes, as it affects the permeability and mechanical properties. The cyrogel membranes were investigated for swelling characteristics. The equilibrium swelling ratio of cryogel membranes is shown in Table 2. Larger cross-linker ratios reduced the size of macropores, thereby reduced the swelling capacity [40].

In vitro delivery studies

The amount of cross linker is another parameter that influences the rate of drug delivery [33]. The MMC delivery behavior from MMC-ICMs at the fixed amount of the drug (100 µg/mL) is shown in Figure 5. As seen in the figure, the cumulative release of MMC decreased by increasing the amount of MBAAm, cross-linker density, in the polymer matrix. The increase of cross-linker density leads to the more rigid and cross-linked structure of cryogel membranes due to contraction and decrease of voids in polymer network. Similar results were also reported in the recent literature [41–43]. For the rest of the drug delivery studies, the MMC-ICM4 was selected because the slowest delivery rate was achieved by this content. This could be due to the increased rigidity of the cryogel in the unfrozen domains as the amount of cross-linker is increased.

Table 3. Release kinetics data for MMC-ICMs.

Notation for cryogels	*n*	k	R^2
MMC-ICM1	0.46	0.71	0.973
MMC-ICM2	0.44	0.7	0.980
MMC-ICM3	0.71	0.54	0.875
MMC-ICM4	0.81	0.32	0.989
MMC-ICM5	0.57	0.06	0.95
MMC-ICM6	0.6	0.12	0.96
MMC-ICM7	0.56	0.33	0.901

The release rate of MMC was studied with different amounts (50, 100 and 200 µg/mL) of template in the MMC-ICM4. As seen in Figure 6, the cumulative release of MMC increased with the increasing amount of MMC. Amount of MMC in cryogel network is directly related to the higher

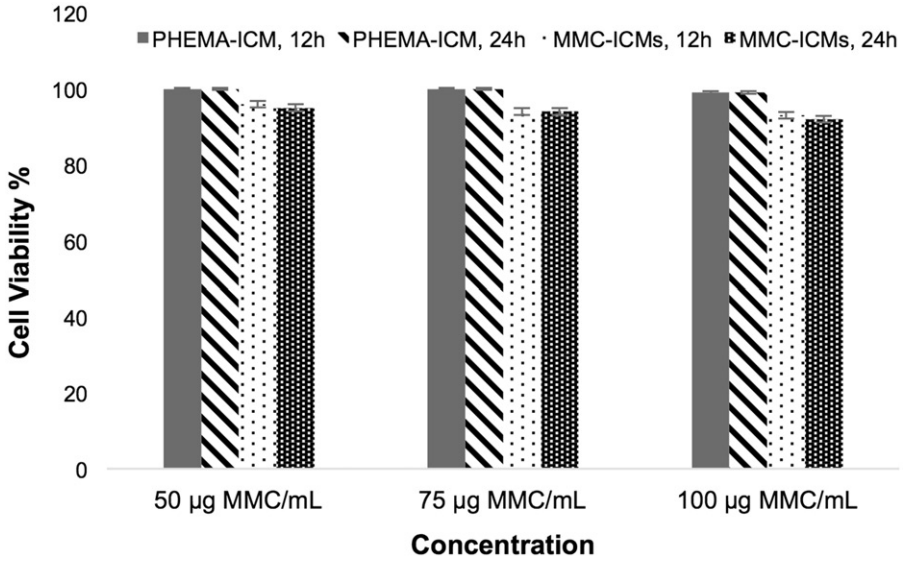

Figure 8. The viability of cell lines treated with MMC-ICMs and PHEMA-ICM (50, 75 and 100 µg MMC/mL) after 12 and 24 h.

diffusion rate of drug molecules from cryogel membranes [33,44]. Cryogels demonstrated very high MMC release efficiency (70–80%) and sustained MMC release over hours ($t = 150$ h).

MMC-ICM was prepared at different polymerization temperatures to examine the effect of temperature on the pore size of the cryogels. The release of MMC was increased by decreasing polymerization temperature. The controlled release of the MMC was slowest for MMC-ICM4 (Figure 7).

To investigate the effect of molecular imprinting of MMC, MMC release from the MMC-ICM4, NICM and PHEMA-ICM were investigated. Results showed that the PHEMA-CMs released most of the loaded drug within 30 min. NICMs showed longer release times due to the metal ion coordination interactions. On the other hand, MMC imprinting resulted in the release of same cumulative amount of drug for much longer times due because of the shape and affinity of the imprinted cavities.

Kinetic studies

The data of *in vitro* drug delivery kinetics and mechanism were analyzed by using Korsmeyer–Peppas models:

$$M\mathrm{t}/\mathrm{M}_{\infty} = \mathrm{k}t^{n} \quad (2)$$

In this equation, "M_t/M_∞" is the fraction of drug delivery, where M_t is the amount of MMC delivery at t time and M_∞ is the MMC delivery at equilibrium time. k is the Korsmeyer–Peppas constant and n is the diffusional expontent in the drug delivery mechanism. The value of n and k were evaluated by fitting the delivery data into the equations. Table 3 shows the constants, MMC delivery exponent data and correlation coefficient (R^2) for cryogel membranes. The correlation coefficient of MMC-ICM4 was the best mechanism of MMC delivery. Following the n values, if $n = 0.5$, the Fickian diffusion is prevailing. If $n > 0.5$, anomalous or non-Fickian diffusion is operative, and for $n = 1$ non-Fickian or case II kinetics occurs. The n values are shown non-Fickian diffusion type for all of the cryogel membranes in this study. Also, k values are decreasing with increasing of cross-linker amount.

In vitro cytotoxicity studies of MMC-ICMs

Cytotoxicity of MMC-ICMs was investigated using mouse fibroblast cell line L929 [7]. The viability of cell lines was determined after 12 and 24 h of the treatment with MMC-ICMs and PHEMA-ICM (50, 75 and 100 µg MMC/mL). The PHEMA-ICM and MMC-ICMs imprinted cryogel membrane were measured as 100.02 ± 0.94 and 98.13 ± 2.89, respectively, after 24 h in 100 µg MMC/mL (Figure 8). These outcomes suggest that the MMC-ICMs may be considered not to be cytotoxic.

Conclusion

In this study, we report the preparation of low cost MMC imprinted cryogel membranes for a local administration of MMC, and their potential for sustained MMC release applications. Cryogels demonstrated very high MMC loading efficiency (70–80%) and sustained MMC release over hours ($t = 150$ h). Due to their interconnected macroporous structures and release kinetics for MMC, the cryogels are useful for controlled cancer therapeutic applications. The drug release was found to be non-Fickian diffusion type for all the cryogel membranes.

Disclosure statement

No potential conflict of interest was reported by the authors.

Funding

Monireh Bakhshpour thanks the Scientific and Technological Research Council of Turkey (TUBITAK) for the support by 'TUBITAK-BIDEB 2215 Programme'.

References

[1] Yavuz H, Çetin K, Akgönüllü S, et al. Therapeutic protein and drug imprinted nanostructures as controlled delivery tools. In: Grumezescu AM, editor. Design and development of new carriers, volume IX sustained and controlled delivery systems part. New York: Elsevier. 2018. p. 439–473 (Chapter 12).

[2] Anselmo AC. An overview of clinical and commercial impact of drug delivery systems. J Control Release. 2014;190:15–28.

[3] Munoz F, Alici G, Li W. A review of drug delivery systems for capsule endoscopy. Adv Drug Deliv Rev. 2014;71:77–85.

[4] Peng H, Dong R, Wang S, et al. A pH-responsive nano-carrier with mesoporous silica nanoparticles cores and poly(acrylic acid) shell-layers: fabrication, characterization and properties for controlled release of salidroside. Int J Pharm. 2013;446:153–159.

[5] Lu CS, Shieh GS, Wang CT, et al. Chemotherapeutics-induced Oct4 expression contributes to drug resistance and tumor recurrence in bladder cancer. Oncotarget. 2017;8:30844–30858.

[6] Goswami MK, Hossain F, Shamsudduha AB, et al. Outcome of intraoperative use of mitomycin C combined with conjunctival auto graft in recurrent pterygium. IMC J Med Sci. 2017;10:49–52.

[7] Öncel P, Çetin K, Topçu AA, et al. Molecularly imprinted cryogel membranes for mitomycin C delivery. J Biomater Sci Polym Ed. 2017;28:519–531.

[8] Kryscio DR, Peppas NA. Mimicking biological delivery through feedback-controlled drug release systems based on molecular imprinting. AIChE J. 2009;55:1311–1324.

[9] Zhang K, Guan X, Qiu Y, et al. A pH/glutathione double responsive drug delivery system using molecular imprint technique for drug loading. Appl Surf Sci. 2016;389:1208–1213.

[10] Chen L, Xu S, Li J. Recent advances in molecular imprinting technology: current status, challenges and highlighted applications. Chem Soc Rev. 2011;40:2922–2942.

[11] Chen L, Wang X, Lu W, et al. Molecular imprinting: perspectives and applications. Chem Soc Rev. 2016;45:2137–2211.

[12] Baydemir G, Denizli A. Heparin removal from human plasma using molecularly imprinted cryogels. Artif Cell Nanomed B. 2015;43:403–412.

[13] Derazshamshir A, Baydemir G, Yılmaz F, et al. Preparation of cryogel columns for depletion of hemoglobin from human blood. Artif Cells Nanomed Biotechnol. 2016;44:792–799.

[14] Göktürk I, Karakoç V, Onur MA, et al. Characterization and cellular interaction of fluorescent-labeled PHEMA nanoparticles. Artif Cell Nanomed B. 2013;41:78–84.

[15] Göktürk I, Perçin I, Denizli A. Catalase purification from rat liver with iron-chelated poly (hydroxyethyl methacrylate-*N*-methacryloyl-(L)-glutamic acid) cryogel discs. Prep Biochem Biotech. 2016a;46:602–609.

[16] Göktürk I, Üzek R, Uzun L, et al. Synthesis of a specific monolithic column with artificial recognition sites for L-glutamic acid via cryo-crosslinking of imprinted nanoparticles. Artif Cells Nanomed Biotechnol. 2016b;44:1133–1140.

[17] Türkoğlu EA, Yavuz H, Uzun L, et al. The fabrication of nanosensor-based surface plasmon resonance for IgG detection. Artif Cells Nanomed Biotechnol. 2013;41:213–222.

[18] Uygun M, Karagözler A, Denizli A. Molecularly imprinted cryogels for carbonic anhydrase purification from bovine ertythrocyte. Artif Cell Nanomed B. 2014;42:128–137.

[19] Kryscio DR, Peppas NA. Critical review and perspective of macromolecularly imprinted polymers. Acta Biomater. 2012;8:461–473.

[20] Wulff G. Molecular imprinting in cross-linked materials with the aid of molecular templates—a way towards artificial antibodies. Angew Chem Int Ed Engl. 1995;34:1812–1832.

[21] Akgönüllü S, Yavuz H, Denizli A. Preparation of imprinted cryogel cartridge for chiral separation of L-phenylalanine. Artif Cell Nanomed B. 2017;45:800–807.

[22] Bakhshpour M, Tamahkar E, Andaç M, et al. Surface imprinted bacterial cellulose nanofibers for hemoglobin purification. Colloids Surf B Biointerfaces. 2017;158:453–459.

[23] Silva MSda, Viveiros R, Morgado PI, et al. Development of 2-(dimethylamino) ethyl methacrylate-based molecular recognition devices for controlled drug delivery using supercritical fluid technology. Int J Pharm. 2011;416:61–68.

[24] Hilt JZ, Byrne ME. Configurational biomimesis in drug delivery: molecular imprinting of biologically significant molecules. Adv Drug Deliv Rev. 2004;56:1599–1620.

[25] Huang J, Hu Y, Hu Y, et al. Disposable terbium (III) salicylate complex imprinted membrane using solid phase surface fluorescence method for fast separation and detection of salicylic acid in pharmaceuticals and human urine. Talanta. 2013;107:49–54.

[26] Lian H, Hu Y, Li G. Novel metal-ion-mediated, complex-imprinted solid phase microextraction fiber for the selective recognition of thiabendazole in citrus and soil samples. J Sep Sci. 2014;37:106–113.

[27] Hiratani H, Mizutani Y, Lorenzo CA. Controlling drug release from imprinted hydrogels by modifying the characteristics of the imprinted cavities. Macromol Biosci. 2005;5:728–733.

[28] Calarco A, Petillo O, Bosetti M, et al. Controlled delivery of the heparan sulfate/FGF-2 complex by a polyelectrolyte scaffold promotes maximal hMSC proliferation and differentiation. J Cell Biochem. 2010;110:903–909.

[29] Türkmen D, Bereli N, Çorman ME, et al. Molecular imprinted magnetic nanoparticles for controlled delivery of mitomycin C. Artif Cell Nanomed B. 2014;42:316–322.

[30] Savina IN, Cnudde V, D'Hollander S, et al. Cryogels from poly(2-hydroxyethyl methacrylate): macroporous, interconnected materials with potential as cell scaffolds. Soft Matter. 2007;3:1176–1184.

[31] Perçin I, Baydemir G, Ergün B, et al. Macroporous PHEMA based cryogel disks for bilirubin removal. Artif Cell Nanomed B. 2013;41:171–177.

[32] Fatoni A, Numnuam A, Kanatharana P, et al. A novel molecularly imprinted chitosan-acrylamide, graphene, ferrocene composite cryogel biosensor used to detect microalbumin. Analyst. 2014;139:6160–6167.

[33] Çetin K, Denizli A. 5-Fluorouracil delivery from metal-ion mediated molecularly imprinted cryogel discs. Colloids Surf B Biointerfaces. 2015;126:401–406.

[34] Çetin K, Perçin I, Denizli F, et al. Tentacle-type immobilized metal affinity cryogel for invertase purification from *Saccharomyces cerevisiae*. Artif Cells Nanomed Biotechnol. 2017;45:1431–1439.

[35] Han ME, Kang BJ, Kim SH, et al. Gelatin-based extracellular matrix cryogels for cartilage tissue engineering. J Ind Eng Chem. 2017;45:421–429.

[36] Göppert B, Sollich T, Abaffy P, et al. Cancer treatment: superporous poly(ethylene glycol) diacrylate cryogel with a defined elastic modulus for prostate cancer cell research. Small. 2016;12:4020.

[37] Caka M, Türkcan C, Uygun DA, et al. Controlled release of curcumin from poly(HEMA-MAPA) membrane. Artif Cells Nanomed Biotechnol. 2017;45:426–431.

[38] Serizawa T, Wakita K, Akashi M. Rapid deswelling of porous poly (*N*-isopropylacrylamide) hydrogels prepared by incorporation of silica particles. Macromolecules. 2002;35:10–12.

[39] Zhang XZ, Zhuo RX. Dynamic properties of temperature-sensitive poly (*N*-isopropylacrylamide) gel cross-linked through siloxane linkage. Langmuir. 2001;17:12–16.

[40] Sayil C, Okay O. Macroporous poly (N-isopropylacrylamide) networks. Poly Bull. 2002;48:499–506.

[41] Babu VR, Sairam M, Hosamani KM, et al. Development of 5-fluorouracil loaded poly(acrylamide-*co*-methylmethacrylate) novel core-shell microspheres: *in vitro* release studies. Int J Pharm. 2006;325:55–62.

[42] Rao KM, Mallikarjuna B, Rao KKSV, et al. Synthesis and characterization of pH sensitive poly (hydroxy ethyl methacrylate-*co*-acrylamidoglycolic acid) based hydrogels for controlled release studies of 5-fluorouracil. Int J Polym Mater Polym Biomater. 2013;62:565–571.

[43] Olukman M, Şanlı O, Solak EK. Release of anticancer drug 5-fluorouracil from different ionically crosslinked alginate beads. Jbnb. 2012;3:469–479.

[44] Das RK, Kasoju N, Bora U. Encapsulation of curcumin in alginate-chitosan-pluronic composite nanoparticles for delivery to cancer cells. Nanomed Nanotechnol Biol Med. 2010;6:153–160.